PTEN DELETION IN SPINAL PATHWAYS VIA RETROGRADE TRANSDUCTION WITH AAV-RG ENHANCES FORELIMB MOTOR RECOVERY AFTER CERVICAL SPINAL CORD INJURY; SEX DIFFERENCES AND LATE-ONSET PATHOPHYSIOLOGIES

Mariajose Metcalfe[a,b], Oswald Steward[a,b,c,d]

[a]Reeve-Irvine Research Center University of California Irvine School of Medicine, USA
[b]Department of Anatomy & Neurobiology, University of California Irvine School of Medicine, USA
[c]Department of Neurobiology & Behavior, University of California Irvine, USA
[d]Department of Neurosurgery, University of California Irvine School of Medicine, USA

Corresponding Author:
Oswald Steward, Ph.D.
Reeve-Irvine Research Center
837 Health Sciences Dr.
University of California Irvine School of Medicine
Irvine, CA 92697
Email: osteward@uci.edu

Keywords: AAV-rg, retrograde transport, corticospinal tract, spinal pathways, AAV-based gene modification, mouse, spinal cord, pathophysiology

Acknowledgements: Supported by NIH grant NS108189 to OS. MM was the recipient of a Career Re-Entry and Diversity Fellowship supplement to NS108189. We gratefully acknowledge generous donations from Cure Medical and Research for Cure. Thanks to Ardi Gunawan for skilled spinal cord surgery, Jamie Mizufuka for superb histological assistance with the immunocytochemistry and analyses, Daniela Gonzalez, Kiara Quinn for assistance in behavioral testing and Kevin Sanchez for assistance in behavioral testing, immunocytochemistry and anatomical analyses.

Author contributions: OS and MM designed the overall project and wrote the paper.

Conflict of interest: OS is a co-founder and has economic interests in the company *Axonis Inc*, a biotechnology which is seeking to develop therapies for spinal cord injury and other neurological disorders.

ABSTRACT

Spinal cord injuries (SCI) cause permanent functional impairments due to interruption of motor and sensory pathways. Regeneration of axons does not occur due to lack of intrinsic growth capacity of adult neurons and extrinsic inhibitory factors, especially at the injury site. However, some regeneration can be achieved via deletion of the phosphatase and tensin homolog (PTEN) in cells of origin of spinal pathways. Here, we deployed an AAV variant that is retrogradely transported (AAV-rg) to deliver gene modifying cargos to the cells of origin of multiple pathways interrupted by SCI, testing whether this promoted recovery of motor function. $PTEN^{f/f}$;$Rosa^{tdTomato}$ mice and control $Rosa^{tdTomato}$ mice received injections of different doses (number of genome copies, GCs) of AAV-rg/Cre into the cervical spinal cord at the time of a C5 dorsal hemisection injury. Forelimb grip strength was tested over time using a grip strength meter. $PTEN^{f/f}$;$Rosa^{tdTomato}$ mice with AAV-rg/Cre (PTEN-deleted) exhibited substantial improvements in forelimb gripping ability in comparison to controls. Of note, there were major sex differences in the extent of recovery, with male mice exhibiting greater recovery than females. However, at around 5-7 weeks post-injury/injection, many mice with SCI and AAV-rg-mediated PTEN deletion began to exhibit pathophysiologies involving excessive scratching of the ears and back of the neck and rigid forward extension of the hindlimbs. These pathophysiologies increased in incidence and severity over time. Our results reveal that although intra-spinal injections of AAV-rg/Cre in $PTEN^{f/f}$;$Rosa^{tdTomato}$ mice can enhance forelimb motor recovery after SCI, late-

63 developing functional abnormalities occur with the experimental conditions used here.

64 Mechanisms underlying late-developing pathophysiologies remain to be defined.

65

66 **1. INTRODUCTION**

67

68 Spinal cord injuries (SCI) interrupt descending motor and autonomic pathways and
69 ascending sensory pathways in the spinal cord, causing paralysis, loss of sensation and
70 loss of bladder and bowel function. Damaged connections within the spinal cord do not
71 regenerate and the prevailing concept is that regeneration failure is due to lack of
72 intrinsic growth capacity of adult neurons and extrinsic inhibitory factors present in the
73 mature nervous system, especially at the injury site.

74 Neuron-intrinsic signaling pathways that enable a regenerative response have been
75 identified. In this context, the phosphoinositide 3-kinase (PI3K)/mechanistic target of
76 rapamycin (mTOR) pathway plays an important role for regulating cell size, protein
77 synthesis, survival and cytoskeleton formation necessary for axon extension after injury
78 (Leibinger et al., 2019; Proud, 2002; Testa and Tsichlis, 2005; Zhou and Snider, 2006).
79 Activation of PI3K via receptor tyrosine kinase (RTK) leads to activation of intracellular
80 serine/threonine protein kinase AKT and downstream activation of the mTOR pathway.
81 Activation of mTOR leads to the phosphorylation of different substrates, including
82 ribosomal protein S6 (pS6), one consequence of which is increased translation of 5'
83 TOP mRNAs important for cell growth (Guertin and Sabatini, 2007). There are other
84 important consequences of mTOR activation in general and S6 phosphorylation in
85 particular including alterations in gene transcription in the nucleus (Proud, 2002).

86 An important negative regulator of the AKT/mTOR pathway is phosphatase and
87 tensin homolog (PTEN), a phosphatase that converts inositol triphosphate (InsP3) to
88 inositol biphosphate (IP2) reversing the action of PI3K. Overall activation of mTOR

89 depends on the balance between PI3K and PTEN, so PTEN inactivation drives the
90 mTOR pathway.

91 Studies from multiple labs have used adeno-associated virus (AAVs) to drive mTOR
92 activity by genetic deletion or knockdown of PTEN delete to enable axon regeneration.
93 AAVs are an effective platform for *in vivo* gene therapy, as they mediate high levels of
94 transgene expression in non-dividing cells, are non-toxic and present low innate
95 immunity (Kaplitt et al., 2007). The initial landmark study deployed AAV2/Cre in PTEN$^{f/f}$
96 mice to delete PTEN in retinal ganglion cells, documenting regeneration with optic nerve
97 crush (Park et al., 2008). Then using PTEN$^{f/f}$ mice and injecting AAV2/Cre into the
98 sensorimotor cortex, un-precedented regeneration of CST axons was documented after
99 SCI (Liu et al., 2010). This has been confirmed in multiple follow-up studies (Danilov
100 and Steward, 2015; Geoffroy et al., 2016; Liu et al., 2010; Willenberg et al., 2016). Of
101 note, the regeneration-enabling effect of PTEN deletion is blocked by rapamycin,
102 implicating mTOR as the critical molecular signaling pathway (Park et al., 2010).
103 Knockdown of PTEN via short-hairpin RNA (shRNA) in the sensorimotor cortex, also
104 enables regeneration of CST axons and enhances motor recovery after injury
105 (Lewandowski and Steward, 2014; Zukor et al., 2013).

106 These studies document that AAV-based delivery of cargos can be effective in
107 enabling regeneration after SCI, but the strategy has been to target one pathway at a
108 time. For example, regeneration of CST axons is enabled by targeting the sensorimotor
109 cortex (Liu et al., 2010) and regeneration of rubrospinal tract axons by targeting the red
110 nucleus (Challagundla et al., 2015). This one pathway at a time approach does not
111 address the critical unmet need for regeneration of multiple pathways following SCI.

112 A potential tool to deliver gene-modifying cargos to the cells of origin of multiple
113 spinal pathways in widely-distributed brain regions comes from the development of the
114 retrogradely transported AAV variant: AAV-rg (Tervo et al., 2016). When injected into
115 the spinal cord, AAV-rg is retrogradely transported to the cells of origin of multiple spinal
116 pathways (Tervo et al., 2016) (Metcalfe et al., 2022; Wang et al., 2018). Here we
117 carried out an initial test of whether AAV-rg-based deletion of PTEN in cells of origin of
118 multiple pathways promotes recovery of motor function. For this, we injected AAV-
119 rg/Cre into the cervical spinal cord in PTEN$^{f/f}$;Rosa^{tdTomato} mice and control Rosa^{tdTomato}
120 mice at the time of a C5 dorsal hemisection injury. Forelimb gripping ability was
121 assessed with a grip strength meter. PTEN$^{f/f}$;Rosa^{tdTomato} mice exhibited greater
122 improvements in forelimb gripping ability in comparison to controls. However, at around
123 5-7 weeks post-injury, some mice began to exhibit pathophysiologies involving
124 excessive scratching and hindlimb dystonia with persistent extension, which increased
125 over time. To begin to assess causes of pathophysiologies, additional studies were
126 carried out to define conditions leading to pathophysiologies. Pathophysiologies were
127 not observed in PTEN$^{f/f}$;Rosa^{tdTomato} mice that received AAV-rg/Cre without concurrent
128 SCI or in PTEN$^{f/f}$;Rosa^{tdTomato} mice that received injections of AAV2/Cre in conjunction
129 with SCI (not AAV-rg/Cre). These results indicate that the pathophysiologies are not due
130 to AAV-rg/Cre mediated deletion alone or selective deletion of PTEN in the spinal cord
131 in conjunction with SCI.
132 Our findings document that although intra-spinal injections of AAV-rg/Cre in
133 PTEN$^{f/f}$;Rosa^{tdTomato} mice can lead to initial improvements in forelimb motor recovery
134 after SCI, there are late-developing functional abnormalities with the experimental

135 conditions used here. The mechanisms underlying late-developing pathophysiologies
136 remain to be defined.
137
138 **2. MATERIALS AND METHODS**
139
140 **2.1 Experimental Animals**
141
142 2.1.1. Animal use and care. All procedures involving animals were approved by the
143 Institutional Animal Care and use Committee (IACUC) of the University of California
144 Irvine in compliance with the National Institute of Health guidelines. Mice were
145 maintained on a 12h light/dark cycle at 25°C. All procedures were done during the light
146 portion of the cycle.
147
148 2.1.2. Mice. Our studies were done using two lines of transgenic mice that we
149 developed in our lab (Gallent and Steward, 2018). One line was created by crossing
150 Rosa26^{tdTomato} mice obtained from the Jackson Laboratory (JAX: 007905) with PTEN$^{f/f}$
151 mice from our breeding colony to create a new transgenic strain that was homozygous
152 at both loci (PTEN$^{f/f}$;Rosa^{tdTomato}). PTEN$^{f/f}$;Rosa^{tdTomato} mice have a lox-P flanked STOP
153 cassette in the ROSA locus and lox-P flanked exon 5 of PTEN so AAV-mediated
154 expression of Cre recombinase deletes PTEN and induces robust expression of
155 tdTomato (tdT) in the same neurons. In creating this new transgenic strain, we also
156 selected for homozygous Rosa^{tdTomato} mice as controls. Because the resulting
157 Rosa^{tdTomato} mice were derived from the crossing, they have a different genetic

158 background from the original, Rosa^{tdTomato} mice obtained from JAX Labs (genetic
159 background B6;129S6).
160
161 2.1.3. AAV vectors: To retrogradely transduce neurons in the brain that project to
162 the spinal cord, we used different AAV-rg vectors in different studies. In studies 1&3
163 (below), AAV-rg/Cre (Addgene viral prep #24593-AAVrg) was used in
164 PTEN$^{f/f}$;Rosa^{tdTomato} mice and control Rosa^{tdTomato} mice. In study 2, which used only
165 PTEN$^{f/f}$;Rosa^{tdTomato} mice, AAV-rg/Cre was used to delete PTEN controls received AAV-
166 rg/GFP (Addgene viral prep #37825-AAVrg). In study 4, mice received AAV-
167 rg/shPTEN/GFP to delete PTEN and controls received similar injections of AAV-rg/Cre.
168 Custom AAV-rg/shPTEN/GFP viral constructs are produced at the University of Pennsylvania
169 Vector Core. The shRNA targeting PTEN has been previously characterized (Lewandowski and
170 Steward, 2014) and it is driven by a human U6 promoter, while, GFP expression is driven by a
171 cytomegalovirus (CMV) promoter. To transduce cells locally within the spinal cord with
172 minimal retrograde transport, Study 5 used AAV2/Cre (Vector Biolabs viral prep #7011).
173
174 **2.2. Spinal cord injuries**
175 Surgical procedures for intra-spinal cord AAV-rg and AAV2 injections at C5 were as
176 previously described (Steward et al., 2021). Mice were anesthetized with Isoflurane (2-
177 3%), their eyes were swabbed with Vaseline, and the skin at the incision site was
178 shaved and cleaned with Betadine. A laminectomy was performed at C5 to expose the
179 underlying spinal cord. Injections (0.3 µl per side) were made using a Hamilton
180 microsyringe fitted with a pulled glass micropipette at 0.5 mm lateral to the midline and
181 0.5 mm deep.

182 C5 dorsal hemisections were performed under the same procedure as intraspinal
183 AAV-rg or AAV2 injections. To create a dorsal hemisection, a 15-degree angled
184 Microscalpel (Electron Microscopy Sciences #72046-15) was inserted into the spinal
185 cord at the midline to a depth of 0.5 mm and drawn laterally, then the blade was turned
186 around and drawn in the opposite direction. This was repeated several times to assure
187 completeness of the dorsal transection. After the spinal cord lesion was created, the
188 mouse was passed to a separate station for AAV injections. After completion of the
189 hemisection and intra-spinal cord AAV injections, muscle layers were sutured and the
190 skin was secured with wound clips.
191

192 **2.3. Post-operative care**

193 Following the surgeries, mice were immediately placed on water-circulating jacketed
194 heating pads at 37°C until they fully recovered from the anesthetic. When able to move
195 around in their cage and feed themselves, mice were housed 2-4 per cage on Alpha-Dri
196 bedding. For 3-5 days post-injury, mice received lactated Ringer solution (1ml/20g, sub-
197 cutaneously) for prophylactic treatment against urinary tract infections. Mice were
198 monitored twice daily for 2 weeks post-injury for general health, coat quality (indicative
199 of normal grooming activity) and mobility within the cage. After this post-operative
200 monitoring, mice were examined by researcher staff at the time of weekly GSM testing
201 and routinely monitored by vivarium staff.
202

203 **2.4. Order of studies to test recovery of function**

204 The overall study of consequences of PTEN deletion on recovery following spinal
205 cord injury (SCI) includes 3 separate studies carried out at different times. Each study
206 involved delivery of different doses of AAV-rg/Cre [dose = number of genome copies
207 (GC) injected per mouse]. For each study, surgeries and AAV-rg/Cre injections were
208 done by the same surgical team and were blind with respect to strain and vector.
209 However, different experimenters were responsible for the functional analyses in each
210 study.

211 Study 1 was performed to determine if PTEN deletion via intra-spinal injection of
212 AAV-rg/Cre would promote functional recovery after SCI. Study 1 involved 15
213 PTEN$^{f/f}$;Rosa^{tdTomato} mice (n=11 male; n=4 female) and 14 control Rosa^{tdTomato} mice (n=4
214 male; n=10 female). Mice were 11 weeks old at the start of the study and were handled
215 for 2 weeks. GSM testing began when mice were 13 weeks of age and continued for 4
216 weeks to collect baseline GSM values. Dorsal hemisection injuries and intra-spinal cord
217 injections of AAV-rg/Cre were done when mice were 17 weeks of age. Mice received 4
218 bilateral injections, 2 above and 2 below the injury (total of 12E9 genome copies (GC)
219 per mouse, 0.3 µl/injection in the same surgery as a dorsal hemisection injury at C5
220 (hemisections were done first). Of those, 3 PTEN$^{f/f}$;Rosa^{tdTomato} mice and 1 Rosa^{tdTomato}
221 mouse died 1-2 days post-surgery. Thus after attrition, starting animal numbers were 12
222 PTEN$^{f/f}$;Rosa^{tdTomato} mice (n=8 male; n=4 female) and 13 Rosa^{tdTomato} mice (n=4 male;
223 n=9 female).

224 Starting 4 weeks post-injury, vivarium staff began reporting wounds behind the ears
225 of many mice. Details on these are described in the Results, as well as our
226 determination of the cause (incessant scratching). Despite treatment, wounds increased

227 in severity to the point that some mice were euthanized. Some mice also began to
228 exhibit rigid forward extension of the hindlimbs, which we term dystonia. Because of the
229 increasing severity of the pathophysiologies, the study was terminated and mice were
230 euthanized 9 weeks post AAV-rg/Cre injections plus SCI.

231 Importantly, mice were group housed (up to 4 mice/cage), treatment groups were
232 not separated, and both vivarium staff and individuals doing GSM testing were blind to
233 genotype. As a result, we did not detect the fact that pathophysiologies were occurring
234 only in $PTEN^{f/f}$;$Rosa^{tdTomato}$ mice with SCI and AAV-rg/Cre until the study was
235 terminated and blinding was removed. Overall, 9/13 $PTEN^{f/f}$;$Rosa^{tdTomato}$ mice with SCI
236 and AAV-rg/Cre exhibited wounds and scratching and some hindlimb dystonia.

237 To begin to define causes of the pathophysiologies, we carried out follow-up studies.
238 In Study 2, we reduced AAV-rg doses (6E9 GC/animal) to determine if this was related
239 to the occurrence of pathophysiologies. Injections were made rostral to the injury rather
240 than both rostral and caudal as in Study 1. Study 2 involved a total of 26
241 $PTEN^{f/f}$;$Rosa^{tdTomato}$ mice that were 11 weeks old at the start of the study. Mice were
242 handled for 2 weeks; GSM testing began when mice were 13 weeks old and continued
243 for 2 weeks to collect baseline GSM values. At 15 weeks of age, mice received dorsal
244 hemisection injuries and bilateral intra-spinal cord injections of AAV above the injury. 16
245 mice (n=9 male; n=7 female) received 6E9 GC per mouse of AAV-rg/Cre. 10 mice (n=6
246 male; n=4 female) received 6E9 GC of the control vector AAV-rg/GFP (0.3 µl/injection).
247 Of those, 9 mice injected with AAV-rg/Cre and 3 mice injected with AAV-rg/GFP died on
248 the first 1-2 days post-surgery. Thus after attrition, starting animal numbers were a total

249 of 18 PTEN$^{f/f}$;Rosa^{tdTomato} mice; 11 mice (n=7 male; n=4 female) injected with AAV-
250 rg/Cre and 7 mice (n=4 male; n=3 female) injected with AAV-rg/GFP.
251 Two PTEN$^{f/f}$;Rosa^{tdTomato} mice injected with AAV-rg/Cre began to exhibit
252 pathophysiologies 5 weeks post injections/SCI, although pathophysiologies were not as
253 severe as seen with higher doses of AAV-rg/Cre in Study 1, and we were able to
254 conduct the experiment to its completion. All mice were perfused 16 weeks post AAV-
255 injection/ SCI.
256 In Study 3 we further reduced AAV-rg dose to 3E9 GC/animal. Here, injections were
257 done rostral to the injury, but only on one side. Onset and nature of pathophysiologies
258 was systematically monitored. Study 3 involved a total of 30 PTEN$^{f/f}$;Rosa^{tdTomato} mice
259 (n=14 male; n=16 female); controls were 16 Rosa^{tdTomato} mice (n=8 male; n=8 female).
260 Mice were 25 weeks old at the start of the study and were handled for 2 weeks. GSM
261 testing began when mice were 27 weeks old and baseline values were collected for 9
262 weeks. At 36 weeks of age, mice received dorsal hemisection injuries and unilateral
263 intra-spinal cord injections of AAV-rg/Cre above the lesion (0.3 µl/injection). 5
264 PTEN$^{f/f}$;Rosa^{tdTomato} mice and 1 Rosa^{tdTomato} mouse died 1-2 days post-surgery, thus
265 after attrition, total starting animal numbers were 25 PTEN$^{f/f}$;Rosa^{tdTomato} mice (n=10
266 male; n=15 female) and 15 Rosa^{tdTomato} mice (n=8 male; n=7 female).
267 Despite lower dose of AAV-rg/Cre, mice in Study 3 still exhibited pathophysiologies
268 (detailed in Results). However, only one mouse was euthanized due to the severity of
269 the pathophysiology, so remaining mice were tested for the planned duration of the
270 study. Mice were perfused 12 weeks post AAV injections/SCI.

271 Study 4 assessed consequences of shRNA-based knockdown of PTEN in
272 conjunction with SCI. 15 Rosa^{tdTomato} mice (n=7 male; n=8 female) received AAV-
273 rg/shPTEN/GFP, while controls were 15 Rosa^{tdTomato} mice that received AAVrg/GFP
274 (n=8 male; n=7 female). Mice were 25 weeks old at the start of the study, were handled
275 for 2 weeks, and then baseline GSM values were collected for 9 weeks. At 34 weeks of
276 age, mice received dorsal hemisection injuries and unilateral intra-spinal cord injections
277 of 3E9 GC per mouse of AAV-rg above the lesion (0.3 µl/injection). 1 mouse injected
278 with AAV-rg/shPTEN/GFP died within the first 2 days post-surgery, and 1 mouse
279 injected with AAV-rg/GFP died 1 day after SCI. Thus, after attrition, starting animal
280 numbers were 14 (n=6 male; n=8 female) for Rosa^{tdTomato} mice injected with AAV-
281 rg/shPTEN/GFP and 14 (n=8 males; n=6 females) for the group injected with AAV-
282 rg/GFP.
283 Of the mice that received AAV-rg/shPTEN/GFP, one male mouse exhibited hindlimb
284 dystonia 1 week post lesion/injection, and excessive scratching. This mouse was
285 euthanized at this time point (1 week post lesion/injection) due to severity of scratching
286 wounds. One male mouse developed shoulder wounds due to scratching 2.5 weeks
287 post lesion/injection and 6 more (n=3 males; n=3 females) began to exhibit
288 pathophysiologies 5 weeks post lesion/injection. The scratching wounds were treated
289 and did not become severe enough to require euthanasia. All other mice continued in
290 the study and were perfused 12 weeks post lesion/injection.
291 Study 5 tested whether pathophysiologies were due to deletion of PTEN in local
292 spinal cord circuitry in the context of a spinal cord injury. For this, mice received
293 AAV2/Cre rather than AAV-rg/Cre at the time of SCI to delete PTEN in the spinal cord

294 around the injection site without retrograde transduction of cells of origin of spinal
295 pathways in the brain. 15 PTEN$^{f/f}$;Rosa^{tdTomato} (n=6 male; n=9 female) and 13
296 Rosa^{tdTomato} mice (n=8 male; n=5 female) were 12 weeks old at the start of the study,
297 were handled for 2 weeks and baseline GSM values were collected for 2 weeks. At 16
298 weeks of age, mice received dorsal hemisection injuries and 2 bilateral intra-spinal cord
299 injections of AAV2/Cre above the injury (0.3 µl/injection). Of these, 1
300 PTEN$^{f/f}$;Rosa^{tdTomato} mouse and 1 Rosa^{tdTomato} mouse died on the first 1-2 days post-
301 surgery; thus after attrition, total starting animal numbers were 14 PTEN$^{f/f}$;Rosa^{tdTomato}
302 mice (n=5 male; n=9 female) and 12 Rosa^{tdTomato} mice (n=8 male; n=4 female). No
303 pathophysiologies were seen, and these mice were perfused 8 weeks post AAV2/Cre
304 injections plus SCI.

305 Several of our previous anatomical studies involved injections of AAV-rg/Cre in
306 PTEN$^{f/f}$;Rosa^{tdTomato} mice and Rosa^{tdTomato} mice without injuries (Metcalfe et al., 2022).
307 Thus, we respectively reviewed husbandry reports and survival statistics to determine
308 whether pathophysiologies occurred with AAV-rg/Cre injections in PTEN$^{f/f}$;Rosa^{tdTomato}
309 mice in the absence of spinal cord injury.

310 The retrospective review included n=12 PTEN$^{f/f}$;Rosa^{tdTomato} mice (n=8 males were
311 between 14-24 weeks old; n=3 females were between 16-24 weeks old). These mice
312 received two bilateral intra-spinal cord injections of AAV-rg/Cre (6E9 GC/mouse) at C5
313 as in study 2 here. No animals died during injection procedures. Mice were allowed to
314 survive for different time periods and were killed for anatomical studies. Two males and
315 1 female mouse were killed 1 month post injection; 4 male mice were killed 4 months
316 post injection; 1 male mouse was killed 7 months post injection and 2 male and 3

317 females were killed 12 months post injection. As detailed in the Results, none of these
318 mice exhibited pathophysiologies.
319 Details on animal use (genotypes, ages at the time of injection, injection location,
320 survival time) are summarized in Table 1.
321
322 **2.5. Grip strength meter (GSM)**
323 The GSM measures grip strength (the maximal peak force in grams) as a mouse is
324 allowed to grip a bar and then is gently pulled away. To test grip strength of one paw,
325 the opposite forepaw is taped with non-stick surgery tape (Danilov and Steward, 2015).
326 For testing, mice were held by the tail and suspended 2-3 inches above the plate of the
327 GSM. Mice were gradually brought toward the bar until they reached out and gripped
328 the bar. Mice were allowed to briefly adjust their paw on the bar to establish grip, then
329 the mice were gently pulled away until the grip was released. The GSM records the
330 maximal force at the time grip was released. This procedure was repeated 4 times in
331 each testing session, recording grip strength separately for each paw and then
332 averaging across the session.
333 For each study, mice were pre-handled for 2 weeks and then pre-trained on the
334 GSM as stated for each study. Mice typically exhibit a stronger grip early in training and
335 then gripping force decreases to a plateau that is maintained over time; consequently,
336 only the last 5 days of pre-injury values are included in the graphs. After GSM training,
337 mice received dorsal hemisections and were then tested post injury on the GSM 3x per
338 week as stated for each study.
339

340 **2.6. Tissue preparation**

341 Mice were transcardially perfused at survival times indicated in Table 1 with 4%
342 paraformaldehyde in 0.1M phosphate buffer (4% PFA). Brains, and spinal cords with
343 attached dorsal root ganglia were dissected, post-fixed in 4% PFA overnight, then
344 immersed in 27% sucrose for cryoprotection overnight, frozen in TissueTek OCT (VWR
345 International) and stored at -20°C until they were sectioned with a cryostat.

346

347 **2.7. Immunostaining to assess AAV transduction**

348 Brains were sectioned at 30 μm in the coronal plane collecting sets of sections at
349 240 μm intervals to generate 10 sets of regularly-spaced sections. One set of the
350 sections was mounted in serial order for visualization of native tdT fluorescence to
351 assess AAV transduction. Other sets of sections were immunostained for tdT (rabbit
352 anti-red fluorescent protein, Rockland Immunochemicals Inc., #600-401-379,
353 RRID:AB_2209751). To assess deletion/knockdown, one set of sections was
354 immunostained for PTEN (rabbit anti-PTEN Cell Signaling Technology #9188L,
355 RRID:AB_2253290). Biotin-conjugated secondary antibodies were used at 1:250
356 dilution and stained with tyramide-Cy3 (for PTEN).

357

358 **2.8. Quantification of PTEN-deleted cortical motoneurons (CMNs)**

359 One set of sections at 240 μm intervals was prepared for PTEN
360 immunofluorescence (IF) to detect PTEN-deleted cortical motoneurons (CMNs). PTEN-
361 deleted neurons appear as unlabeled “ghost-cells” against the background fluorescence
362 over the neuropil. In $PTEN^{f/f}$;$Rosa^{tdTomato}$ mice, neurons transduced by AAV-rg/Cre

363 express tdTomato (tdT), and native tdT fluorescence is visible in sections prepared for
364 PTEN immunofluorescence allowing co-imaging, which confirmed that tdT-positive
365 neurons also negative for PTEN (Fig. 1).
366 Ten sections spanning 2.4 mm along the A-P axis were used for quantitative
367 analyses of numbers of PTEN-deleted neurons (ghost cells). For animals in the high
368 dose group (12E9 GC/mouse), n=4 mice were chosen taking the first three in the study
369 list that were not used for analyses for other studies (Metcalfe et al., 2022). For mid
370 doses (6E9 GC/mouse) n=2 mice were chosen from the top and the bottom of the study
371 list and that survived until the end of the study. The area of each section containing
372 PTEN-deleted neurons was imaged at 10X. Images of cortex containing ghost cells
373 were obtained by setting edge points encompassing the totality of layer V in that section
374 at 10x magnification using the Keyence microscope "Image Stitch" program. Keyence
375 analysis software stitched the individual frames together and measurements were then
376 exported to ImageJ (Schneider et al., 2012) to determine the average number of PTEN-
377 negative neurons (ghost cells) per section and then average number of ghost-cells per
378 mouse. Measurements were then exported to Excel (Microsoft) and an average of
379 ghost-cells per mouse for each dose was determined.
380
381 **2.9. Statistical Analyses**
382 Prism software was used for all statistical analyses. For statistical analysis of ghost
383 cells numbers, the analysis was a one-way ANOVA with a post hoc Tukey's multiple
384 comparisons test to determine significant differences among groups. For GSM values
385 analyses, the primary statistical analysis was by a two-way repeated measures ANOVA

386 for each separate study with variables of "groups" and "time post-injury". A mixed
387 effects model analysis was used when values were missing for some timepoints,
388 particularly when animals were euthanized due to health concerns. We also calculated
389 *percent recovery in each group* by comparing average pre-injury GSM values vs. peak
390 post injury values. Statistical analyses then compared groups (PTEN deleted vs.
391 control) with values being the percent recovery for each animal.
392
393 **3. RESULTS**
394
395 **3.1 Intra-spinal cord injections of AAV-rg/Cre in PTEN$^{f/f}$;Rosa^{tdTomato} mice**
396 **transduce corticomotor neurons to induce tdT expression and delete PTEN**
397
398 The present study takes advantage of a model using double-transgenic mice
399 (PTEN$^{f/f}$;Rosa^{tdTomato}) and AAV-rg/Cre, which allows remote transduction of neurons via
400 retrograde transport. We have previously shown that intra-spinal cord injections of AAV-
401 rg/Cre in PTEN$^{f/f}$;Rosa^{tdTomato} mice led to selective transduction of thousands of neurons
402 in layer V of the sensorimotor cortex as revealed by induction of tdTomato (tdT)
403 expression. These are the cells of origin of the corticospinal tract (CST), termed
404 “corticomotor neurons” (CMNs). Cells of origin of other descending spinal pathways
405 were also transduced, including neurons in the brainstem reticular formation, red
406 nucleus, and hypothalamus (Metcalfe et al., 2022). Studies from other groups have
407 revealed that AAV-rg also transduces the cells of origin of some but not all intra-spinal
408 circuits; for example, neurons of the propriospinal pathways and serotoninergic neurons

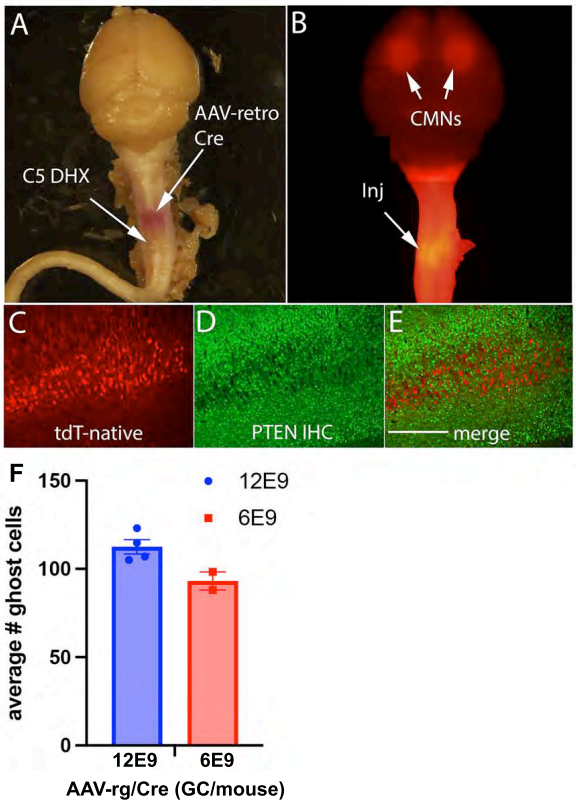

in the midline raphe nuclei of the medulla are not efficiently transduced (Wang et al., 2018). Finally, some populations of neurons in dorsal root ganglia near the injection are also transduced (Metcalfe et al., 2022).

Results of the present studies were consistent with previous data. In Study 1, PTEN$^{f/f}$;Rosa^{tdTomato} mice received doses of AAV-rg/Cre that were 2-fold higher than in our previous study (total of 12E9 GC/mouse) at the time of a dorsal hemisection. This

Figure 1. Retrograde transfection of cortical motoneurons (CMNs) with injections of retro-AAV/Cre into the spinal cord of PTEN$^{f/f}$: Rosa^{tdTomato} mice. A) Intact brain and attached spinal cord. tdTomato is visible at the site of injection in the cervical spinal cord as well as the site of injury (arrows) B) Epifluorescence images of the same brain and spinal cord showing oval areas of tdT fluorescence marking clouds of CMNs expressing tdT and site of injection in thecervical spinal cord (arrows). C-E) Coronal sections through the sensorimotor cortex showing large numbers of native fluorescent tdT-positive pyramidal neurons in layer V (C) that were completely negative for PTEN protein (D). Co-imaging for tdT revealed that tdT-positive neurons are negative for PTEN protein (E). F) Different doses of AAV-retro/Cre revealed an average of 112.5 ghost cells/section at the 12E9 GC dose, 93.16 ghost cells per section at the 6E9 GC/mouse dose, and 42.7 ghost cells at the 3E9 dose. One-way ANOVA revealed significant differences between GC doses [F(64.96) DF 2, 6, p<0.0001]. Post-hoc Tukey's multiple comparisons test revealed significant differences between high (12E9 GC/mouse) and low GC doses (3E9 GC/mouse) (p<0.0001, 95% C.I. = [46.6, 81.27] and between intermediate (6E9 GC/mouse) and low GC doses (3E9 GC/mouse) (p = 0.0014, 95% C.I. = [23.88, 65.32]). There were no significant differences between high (12E9 GC/mouse) and intermediate GC doses (6E9 GC/ml) (p = 0.0532, 95% C.I. = [-0.32, 39]).

was delivered in 4 injections, 2 above and 2 below the injury. TdT was visible in the spinal cord at the injection site in intact spinal cords (Fig. 1A), and epi-fluorescence illumination revealed oval areas of tdT fluorescence in the cortex marking clouds of CMNs expressing tdT (Fig. 1B). In coronal sections through the sensorimotor cortex,

424 large numbers of tdT-positive pyramidal neurons were evident in layer V without
425 immunostaining (native fluorescence, Fig. 1C).
426 Confirming previous findings, immunostaining for PTEN in PTEN$^{f/f}$;Rosa^{tdTomato} mice
427 injected with AAV-rg/Cre revealed large numbers of CMNs that were completely
428 negative for PTEN protein, appearing as "ghost cells" (Fig. 1D, same section as Fig.
429 1C). Co-imaging for tdT revealed that tdT-positive neurons are negative for PTEN
430 protein (No double labeling, which would be represented in yellow, Fig. 1E).
431 Different doses of AAV-rg/Cre were delivered in studies 1, 2, and 3 (12E9
432 GC/mouse delivered in two injections above the lesion in study 1, 6E9 GC/mouse
433 delivered in two injections above the lesion in study 2, and 3E9 GC/mouse in one
434 unilateral injection in Study 3). Counts revealed an average of 112.5 ghost cells/section
435 throughout the sensorimotor cortex at the 12E9 GC dose and 93.16 ghost cells per
436 section at the 6E9 GC/mouse dose (Fig. 1F). Mice in study 3 received intra-cortical BDA
437 injections prior to sacrifice, which cause some cortical damage, making the tissue
438 unsuitable for counts of ghost cells. Two-tailed t-test analysis revealed significant
439 differences between high (12E9 GC/mouse) and intermediate GC doses (6E9 GC/ml)
440 ($t(4.00) = 2.790$, $p = 0.0454$). The likely explanation for the small difference between the
441 high and intermediate GC doses in average numbers of PTEN-negative cells/section is
442 that 2 of the injections at the high dose were below the injury. With complete dorsal
443 hemisections, injections below the injury would not be expected to transduce many
444 CMNs because the dorsal and dorso-lateral CST is completely transected.
445

446 **3.2. Enhanced recovery of forelimb motor function after SCI with intra-spinal**
447 **cord injections of AAV-rg/Cre**
448
449 3.2.1. Study 1:
450 The rationale of Study 1 was to test AAV-rg as a platform to delete PTEN in multiple
451 descending and ascending pathways that would be transected by a dorsal hemisection
452 injury. For this, mice received dorsal hemisection injuries at C5 and bilateral injections
453 of AAV-rg/Cre 1mm rostral and 1mm caudal to the injury (total of 12E9 GC/mouse).
454 Controls were $Rosa^{tdTomato}$ mice that received comparable injections. Forelimb motor
455 function was assessed over time using a GSM by an individual blinded to treatment
456 group.
457 Following C5 lesions and AAV-rg/Cre intra-spinal cord injections, GSM values
458 dropped after injury to 5.5% of pre-injury values for $Rosa^{tdTomato}$ mice and 26.9% of pre-
459 injury values for $PTEN^{f/f}$;$Rosa^{tdTomato}$ mice (Fig. 2A). For the control $Rosa^{tdTomato}$ mice
460 GSM values recovered to a plateau at around 14 days (36% of pre-injury control). In
461 contrast, values for $PTEN^{f/f}$;$Rosa^{tdTomato}$ mice increased progressively reaching a
462 plateau at 25 days of 84% of pre-injury control values. At all post-injury time points,
463 average values for the $PTEN^{f/f}$;$Rosa^{tdTomato}$ mice (PTEN-deleted) were higher than
464 $Rosa^{tdTomato}$ controls. Two-way repeated measures ANOVA revealed significant
465 differences over time [F(15.13) DF 18, 414, $p<0.0001$] and between genotypes [F(6.41)
466 = DF 1,23, $p=0.018$].
467
468 3.2.1.a. Comparisons by sex:

469 Stratification of GSM data by sex (Fig. 2B &C) revealed no sex differences in the
470 values of the Rosa^{tdTomato} control mice. However, there were substantial sex differences
471 in PTEN$^{f/f}$;Rosa^{tdTomato} mice (PTEN-deleted). Specifically, enhanced recovery of GSM
472 values was seen primarily in male mice. GSM values for female PTEN$^{f/f}$;Rosa^{tdTomato}
473 mice (PTEN-deleted) were 77.3% of pre-injury control at the plateau vs. 35.6% for the
474 Rosa^{tdTomato} female control mice. In contrast, GSM values for male PTEN$^{f/f}$;Rosa^{tdTomato}
475 mice were 95.6% of pre-injury control at the plateau vs. 27.1% for the Rosa^{tdTomato} male
476 control mice. Two-way repeated measures ANOVA revealed no significant sex
477 differences for the Rosa^{tdTomato} mice [F(0.63) DF 1,11, p=0.442] but significant sex
478 differences for the PTEN$^{f/f}$;Rosa^{tdTomato} mice [F(4.97) DF 1,10, p=0.05]. Thus, the values
479 for the male PTEN$^{f/f}$;Rosa^{tdTomato} mice largely accounted for the overall difference in the
480 combined values reported above.
481
482 <u>3.2.1.b. Late-developing pathophysiologies:</u>
483 Mice were tested with GSM once/week and after the initial post-injury period; mice
484 were not individually examined every day by research staff but were monitored routinely
485 by vivarium staff (routine animal husbandry). At 4 weeks post-injury, vivarium staff
486 reported a mouse with severe skin wounds behind the ears and on the neck. These
487 wounds were initially attributed to “over-grooming”. After careful observation, we
488 determined that the mouse was repeatedly scratching the area of the wound with its
489 hindlimbs. Wounds on this mouse were severe so the mouse was euthanized. At 5
490 weeks, another mouse was reported as having wounds diagnosed as “ulcerative
491 dermatitis”. Wounds were treated with Silvadeen and toenails were trimmed. Similar

492 wounds began to appear in other mice that were attributed to various causes; in each
493 case, wounds were treated with Silvadeen and toenails were trimmed. At 6 weeks, 3
494 more mice exhibited wounds that were diagnosed as “skin lesions” and “ulcerative
495 dermatitis”. At 7 weeks, 2 more mice exhibited wounds that were diagnosed as “fight
496 wounds and ulcerative dermatitis”. Finally, at 9 weeks, 2 more mice exhibited wounds
497 diagnosed as “fight wounds” in one case and “ulcerative dermatitis” in the other. Some
498 mice also began to exhibit rigid forward extension of the hindlimbs, which we term
499 dystonia. Figure 3 illustrates the nature of these late-onset pathophysiologies.
500 Overall, 9/13 PTEN$^{f/f}$;Rosa^{tdTomato} mice with SCI and AAV-rg/Cre exhibited wounds
501 and scratching. We had originally planned to inject BDA to trace CST axons, but
502 because of the continued incessant scratching and increasing severity of the wounds,
503 we terminated the experiment and all remaining mice were euthanized and perfused at
504 64 days post- AAV-rg/Cre injections. When mice were terminated, we did not note the
505 sex of mice that had exhibited pathophysiologies, and whether there were sex
506 differences in the incidence or severity of wounds.
507
508 <u>3.2.2. Study 2:</u>
509 To begin to define causes and mechanisms of the pathophysiologies that appeared
510 in study 1, in study 2, we made 2 adjustments to the dosing. First, the overall dose was
511 reduced to 6E9 GC/mouse to determine whether this dose could promote forelimb
512 recovery without occurrence of pathophysiologies. Second, because some mice
513 exhibited rigid forward extension of the hindlimb, we wondered whether this would be
514 reduced or eliminated if AAV-rg/Cre injections were only rostral to the injury. Also, for

515 controls, genotype was held constant; all mice were PTEN$^{f/f}$;Rosa^{tdTomato} but the control
516 group was injected with AAV-rg/GFP rather than AAV-rg/Cre.
517 One week following C5 lesions and AAV-rg injections, GSM values on the first
518 testing day were 1% of pre-injury values for mice injected with AAV-rg/Cre and 1.7% of
519 pre-injury values for mice injected with AAV-rg/GFP. For the control mice injected with
520 AAV-rg/GFP, GSM values recovered progressively to a plateau at around 25 days post-
521 injury (9.1% of pre-injury control). In contrast, values for PTEN-deleted mice increased
522 progressively reaching a plateau at 25 days 49.3% of pre-injury control values (Fig. 2D).
523 A mixed effects model analysis revealed significant differences over time [F(121.1) DF
524 5.07, 65.4, $p<0.0001$] and between genotypes [F(5.47) = DF 1, 14, $p=0.035$].
525 Of note, post-injury values for controls were lower in this study (9% of pre-injury) in
526 comparison to study 1 (36% of pre-injury). One possible explanation is that the control
527 group is differs between studies (Rosa^{tdTomato} in study 1 vs. PTEN$^{f/f}$;Rosa^{tdTomato} that
528 received AAV-rg/GFP in study 2). Differences in lesion extent are possible but less likely
529 because the same surgeon did the dorsal hemisections for all studies. The other
530 possibility is that different researchers tested mice by GSM in the two studies. Because
531 of the differences in GSM testers between study 1 and 2 we defined more strict criteria
532 for GSM scoring to improve inter-rater reliability for subsequent studies.

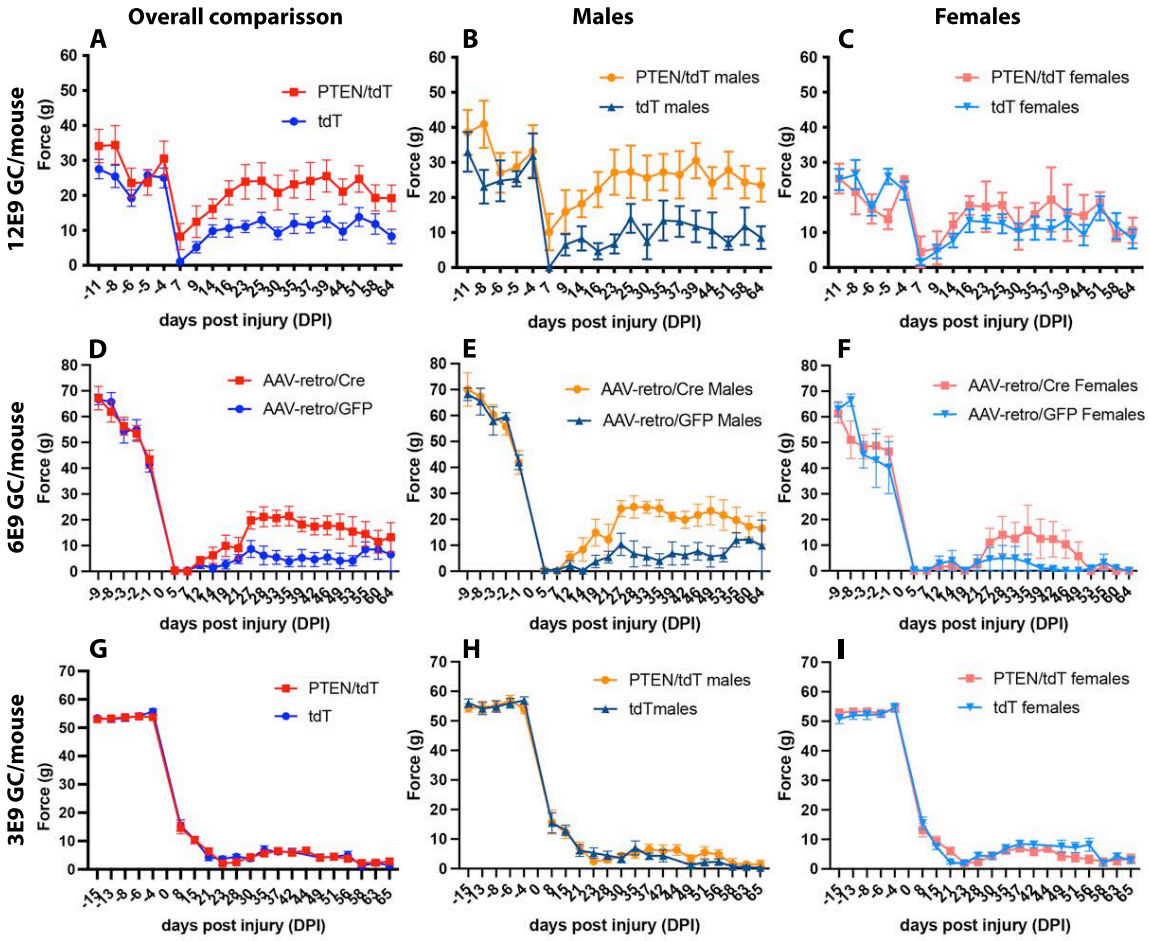

533

Figure 2. Genetic deletion of PTEN promotes transient functional recovery followed by functional deterioration. Forepaw gripping function as measured by grip strength meter (GSM). A) Rosa^{tdTomato} and PTEN$^{f/f}$;Rosa^{tdTomato} mice were injected with 12E9 GC/mouse of AAV-retro/Cre at the same time as a cervical dorsal hemisection. Two-way repeated measures ANOVA revealed significant differences over time [F(15.13) DF 18, 414, p<0.0001] and between genotypes [F(6.41) = DF 1,23, p=0.018]. B-C) Stratification of GSM data by sex revealed no sex differences in the values of the Rosa^{tdTomato} control mice [F(0.63) DF 1,11, p=0.442], whereas there were substantial sex differences in PTEN$^{f/f}$;Rosa^{tdTomato} mice (PTEN-deleted) [F(4.97) DF 1,10, p=0.05]. D) PTEN$^{f/f}$;Rosa^{tdTomato} mice were injected with 6E9 GC/mouse of AAV-retro/Cre or AAV-retro/GFP at the same time as a cervical dorsal hemisection. A mixed effects model analysis revealed significant differences over time [F(121.1) DF 5.07, 65.4, p<0.0001] and between genotypes [F(5.47) = DF 1, 14, p=0.035]. E-F) Stratification of GSM data by sex revealed no sex differences in the values of the AAV-retro/GFP control mice (PTEN intact) [F(1.63) DF 1,5, p=0.26] but significant sex differences for the PTEN-deleted mice injected with AAV-retro/Cre [F(8.39) DF 1,7, p=0.023]. G) Rosa^{tdTomato} and PTEN$^{f/f}$;Rosa^{tdTomato} mice were injected with 3E9 GC/mouse of AAV-retro/Cre at the same time as a cervical dorsal hemisection. A mixed effects model analysis revealed significant differences over time [F(823.0) DF 4.56, 174.6, p<0.0.001] but no significant differences between genotypes [F(0.018) = DF 1, 39, p=0.8944]. H-I) A mixed model ANOVA revealed no significant sex differences for the Rosa^{tdTomato} mice [F(0.92) DF 1,13, p=0.35] nor for the PTEN$^{f/f}$;Rosa^{tdTomato} mice [F(2.29) DF 1,23, p=0.63].

534

535 3.2.2.a. Comparisons by sex:

536 Stratification of GSM data by sex (Fig. 2E &F) revealed no sex differences in the
537 values of the AAV-rg/GFP control mice (PTEN intact). However, as in Study 1, there
538 were substantial sex differences in PTEN$^{f/f}$;Rosa^{tdTomato} mice injected with AAV-rg/Cre
539 (PTEN-deleted). Again, enhanced recovery of GSM values was greater in male mice.
540 GSM values for female PTEN-deleted were 30.25% of pre-injury control at the plateau
541 vs. 7.86% for the PTEN-intact female control mice. In contrast, GSM values for male
542 PTEN-deleted mice were 61.1% of pre-injury control at the plateau vs. 11.8% for the
543 PTEN-intact male control mice. A mixed effects model analysis revealed no significant
544 sex differences for control mice injected with AAV-rg/GFP [F(1.63) DF 1,5, p=0.26] but
545 significant sex differences for the PTEN-deleted mice injected with AAV-rg/Cre [F(8.39)
546 DF 1,7, p=0.023]. Thus, as in study 1, the values for the male PTEN$^{f/f}$;Rosa^{tdTomato} mice
547 largely accounted for the overall difference in the combined values.

548

549 3.2.2.b. Late-developing pathophysiologies:

550 Although mice that received AAV-rg/Cre exhibited higher GSM scores throughout
551 the testing period, pathophysiologies developed at 5 weeks post injection/SCI in n=2
552 PTEN$^{f/f}$;Rosa^{tdTomato} mice (n=1 male; n=1 female). The male mouse was reported as
553 having hindlimb dystonia plus autophagia and the female exhibited scratching wounds
554 on shoulders. These mice were euthanized because of the severity of the wounds.
555 Behavioral testing (GSM) continued for 64 days for the remaining mice [7
556 PTEN$^{f/f}$;Rosa^{tdTomato} mice injected with AAV-rg/Cre (n=5 male; n=2 female) and 7

557 injected with AAV-rg/GFP (n=4 male; n=3 female)]. We did not record which animal
558 numbers exhibited pathophysiologies, so in this study we were unable to determine if
559 there were sex differences in the incidence of wounds. None of the controls
560 (PTEN$^{f/f}$;Rosa^{tdTomato} mice injected with AAV-rg/GFP, PTEN-intact) exhibited excessive
561 scratching, wounds, or hindlimb dystonia at any time. Mice were perfused 16 weeks
562 post injection/SCI.

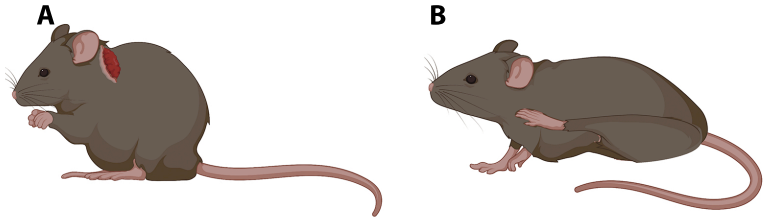

Figure 3. Pathophysiology with AAV-rg mediated PTEN deletion and SCI. At 2-3 months post-injury animals develop excessive scratching and hindlimb dystonia. PTEN$^{f/f}$;Rosa^{tdTomato} injected with AAV-rg/Cre show severe scratching (A) and/or hindlimb dystonia (B).

563

564 <u>3.2.3. Study 3:</u>

565 In study 3 we further decreased AAV-rg/Cre doses (3E9 GC/animal).
566 PTEN$^{f/f}$;Rosa^{tdTomato} mice received 1 unilateral injection above the level of the dorsal
567 hemisection at approximately C4. Controls were Rosa^{tdTomato} mice that received
568 comparable injections. Forelimb motor function was assessed over time using a GSM
569 by an individual blinded to treatment group.

570 Following C5 lesions and AAV-rg/Cre injections, (one week post-injury), GSM values
571 decreased to 4.1% of pre-injury values for Rosa^{tdTomato} mice and 6.4% of pre-injury
572 values for PTEN$^{f/f}$;Rosa^{tdTomato} mice. For the control Rosa^{tdTomato} mice GSM values
573 recovered to a plateau at around 25 days post-injury (6.8% of pre-injury control). Values
574 for PTEN$^{f/f}$;Rosa^{tdTomato} mice were slightly higher than control mice, reaching a plateau
575 at 25 days 12.4% of pre-injury control values (Fig. 2G). A mixed effects model analysis

revealed significant differences over time [F(823.0) DF 4.56, 174.6, p<0.0.001] but no significant differences between genotypes [F(0.018) = DF 1, 39, p=0.8944]. Since injections were unilateral, we analyzed GSM values per paw (right and left). A mixed effects model analysis revealed significant differences over time on the left [F(470.2) DF 5.14, 197.9, p<0.0.001] and the right paw [F(606.7) DF 6.79, 261.5, p<0.0.001] but no significant differences between genotypes on the left [F(0.545) DF 1, 40, p=0.465] or the right paw [F(0.00059) = DF 1, 40, p=0.981] (Fig. 4).

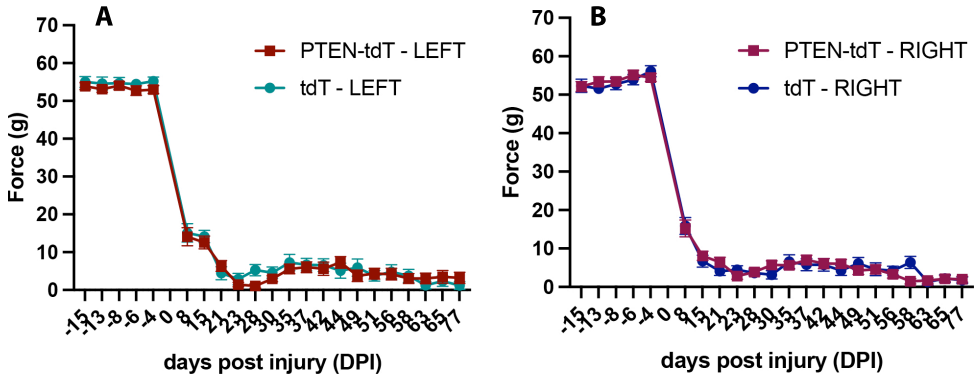

Figure 4. Unilateral low doses of AAV-rg/Cre show no difference in paw performance. Since injections were unilateral, we analyzed GSM values per paw (right and left). A mixed effects model analysis revealed significant differences over time on the left [F(470.2) DF 5.14, 197.9, p<0.0.001] and the right paw [F(606.7) DF 6.79, 261.5, p<0.0.001] but no significant differences between genotypes on the left [F(0.545) DF 1, 40, p=0.465] or the right paw [F(0.00059) = DF 1, 40, p=0.981] (Fig. 4).

<u>3.2.3.a. Comparisons by sex:</u>

Stratification of GSM data by sex (Fig. 2H &I) revealed no sex differences in the values of the Rosa^{tdTomato} control mice or PTEN$^{f/f}$;Rosa^{tdTomato} mice (PTEN-deleted). Specifically, GSM values for female PTEN$^{f/f}$;Rosa^{tdTomato} mice (PTEN-deleted) were 12.6% of pre-injury control at the plateau vs. 15.6% for the Rosa^{tdTomato} female control mice. GSM values for male PTEN$^{f/f}$;Rosa^{tdTomato} mice were 13% of pre-injury control at the plateau vs. 7.7% for the Rosa^{tdTomato} male control mice. A mixed model ANOVA

592 revealed no significant sex differences for the Rosa^{tdTomato} mice [F(0.92) DF 1,13,
593 p=0.35] nor for the PTEN$^{f/f}$;Rosa^{tdTomato} mice [F(2.29) DF 1,23, p=0.63]. Overall neither
594 group showed improvement in recovery of function after SCI plus AAV-rg/Cre injection.
595 Again, post-injury values for controls were lower in this study (6.8% of pre-injury) in
596 comparison to study 1 (36% of pre-injury). In this case, the control group is the same
597 (Rosa^{tdTomato}). Differences in lesion extent are possible but less likely because the same
598 surgeon did the dorsal hemisections for all studies. The possible explanation that
599 remains is that the GSM tester in study 1 was different than in studies 2 and 3.
600
601 <u>3.2.3.b. Late-developing pathophysiologies:</u>
602 In study 3, despite lowering the dose of AAV-rg/Cre to the extent that functional
603 recovery due to PTEN deletion was lost, PTEN$^{f/f}$;Rosa^{tdTomato} mice (PTEN-deleted) mice
604 still developed late occurring pathophysiologies. The first incidence of pathophysiology
605 was reported 3 weeks post AAV-rg/Cre injection and SCI in n=4 mice (all males). N=3 of
606 those showed injuries behind their ears due to chronic scratching and n=1 exhibited
607 hindlimb dystonia. Of those, 1 of the animals that were scratching subsequently
608 developed hindlimb dystonia at 7 weeks post AAV-rg/Cre injections plus SCI. This
609 mouse was euthanized due to severity of injuries at this time point. New cases of
610 pathophysiologies appeared at 7 weeks post AAV-rg/Cre injections plus SCI in n=9
611 mice (n=5 males; n=4 females). Of these, n=4 showed only scratching behind the ears,
612 n=1 only hindlimb dystonia and n=4 exhibited both scratching and hindlimb dystonia.
613 Injuries were not as severe as in study 1, so no other animals were euthanized due to
614 severity of pathophysiologies. Thus out of n=26 PTEN$^{f/f}$;Rosa^{tdTomato} mice (n=10 males;

615 n=16 females), 8/10 males and 5/16 females developed pathophysiologies starting 3
616 weeks post AAV-rg/Cre injections plus SCI, These results suggest that the incidence of
617 pathophysiologies in males is higher compared to females. Animals were perfused 12
618 weeks post AAV-rg/Cre injections plus SCI.
619
620 3.2.4. Study 4: AAV-rg/shRNA-based knockdown of PTEN:
621 Study 4 assessed whether PTEN knockdown via AAV-rg/shPTEN would enhance
622 motor recovery and/or lead to pathophysiologies. Rosa^{tdTomato} mice received unilateral
623 intraspinal cord injections of AAV-rg/shPTEN/GFP above the injury (3E9 GC/mouse).
624 Controls were Rosa^{tdTomato} mice that received similar injections of AAV-rg/Cre. Forelimb
625 motor function was assessed over time using a GSM by an individual blinded to
626 treatment group.
627 Following C5 lesions and AAV-rg injections, GSM values were 8% of pre-injury
628 values at 21 days post-injury for mice injected with AAV-rg/Cre (PTEN-intact controls).
629 Earlier time points are not shown because of errors in scoring. Values for mice that
630 received AAV-rg/shPTEN were 5% of pre-injury control. For the control PTEN-intact
631 mice GSM values recovered to a plateau at around 37 days post-injury of 11.8% of pre-
632 injury control, whereas values for Rosa^{tdTomato} mice that received AAV-rg/shPTEN were
633 6.7% of pre-injury control. A mixed effects model analysis revealed significant
634 differences over time [F(535.8) DF 25, 375, p<0.0.001] and but no significant
635 differences between PTEN-deleted and PTEN-intact groups [F(0.8753) = DF 1, 15,
636 p=0.4301] (Fig. 5A).
637

638 3.2.4.a. Comparisons by sex:

639 Stratification of GSM data by sex (Fig. 5B &C) revealed no sex differences in the
640 values of the Rosa^{tdTomato} control mice injected with AAV-rg/Cre and injected with AAV-
641 rg/shPTEN/GFP. GSM values for female mice that received AAV-rg/shPTEN were
642 4.68% of pre-injury control at the plateau vs. 18.9% for the Rosa^{tdTomato} female control
643 mice. GSM values for male mice that received AAV-rg/shPTEN were 9.57% of pre-
644 injury control at the plateau vs. 4.8% for the Rosa^{tdTomato} male control mice. A mixed
645 effects model analysis revealed no significant sex differences for the control Rosa^{tdTomato}
646 mice [F(0.079) DF 1,13, p=0.78] nor for the Rosa^{tdTomato} mice injected with AAV-
647 rg/shPTEN/GFP (PTEN-knockdown) [F(0.11) DF 1,12, p=0.74]. Overall neither sex
648 showed improvement in recovery of function after SCI plus AAV-rg/shPTEN/GFP
649 injection.

650

651 3.2.4.b. Late-developing pathophysiologies:

652 Although mice with AAV-rg/shPTEN/GFP (PTEN knock-down) did not show
653 improvements in motor function in comparison to controls, they did develop
654 pathophysiologies. One male mouse that received AAV-rg/shPTEN/GFP exhibited
655 hindlimb dystonia 1-week post-surgery. This animal was euthanized due to lack of
656 mobility and health concerns. One male mouse that received AAV-rg/shPTEN/GFP
657 exhibited shoulder wounds due to scratching 2.5 weeks post AAV-rg/shPTEN
658 intraspinal injection plus SCI. N=6 mice showed pathophysiologies 5 weeks post AAV-
659 rg/shPTEN/GFP intraspinal injection plus SCI. Of those 6, n=5 (n=3 males; n=2
660 females) exhibited only dystonia and n=1 (female) exhibited both scratching and

dystonia. Of those 6 animals, one mouse was euthanized due to the severity of the scratching wounds. Scratching wounds were treated with Silvadeen and toenails were trimmed. Of n=14 Rosa^{tdTomato} mice (n=6 males; n=8 females), n=8 developed pathophysiologies starting 1 week post AAV-rg/shPTEN/GFP intraspinal injection plus SCI. Of those 8, n=5 were males and n=3 were females; therefore, there was no apparent sex difference in incidence of pathophysiologies with AAV-rg/shPTEN/GFP injections plus SCI. Animals were perfused 12 weeks post AAV-rg/shPTEN/GFP injections plus SCI.

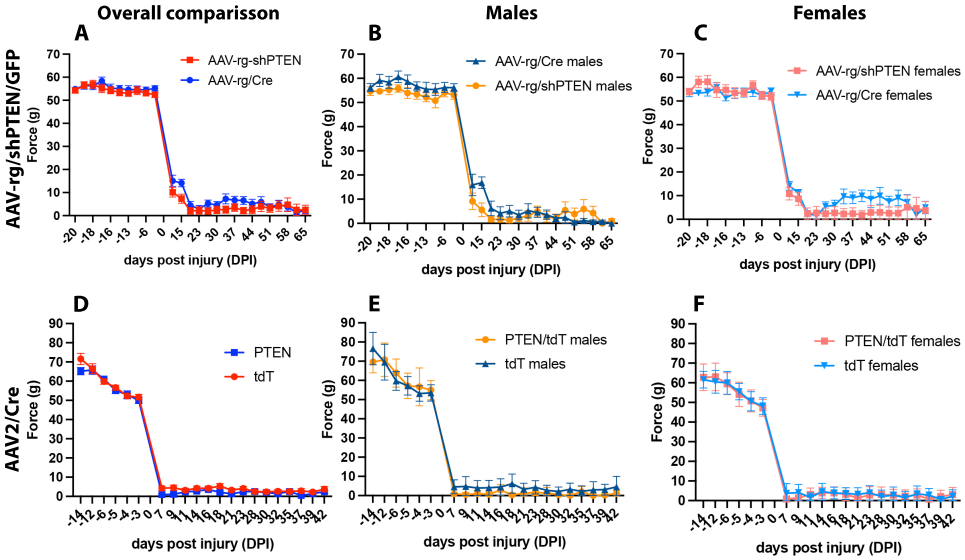

Figure 5. PTEN knockdown with AAV-rg/shPTEN/GFP and PTEN deletion in local spinal circuitry does not promotes functional recovery. Forepaw gripping function as measured by grip strength meter (GSM). A) Rosa^{tdTomato} mice were injected with 3E9 GC/mouse of AAV-rg/shPTEN/GFP or AAV-rg/Cre at the same time as a cervical dorsal hemisection. A mixed effects model analysis revealed significant differences over time [F(535.8) DF 25, 375, p<0.0.001] and but no significant differences between genotypes [F(0.8753) = DF 1, 15, p=0.4301]. B-C) A mixed effects model analysis revealed no significant sex differences for the control Rosa^{tdTomato} mice [F(0.079) DF 1,13, p=0.78] nor for the Rosa^{tdTomato} mice injected with AAV-retro/siPTEN/GFP (PTEN-knockdown) [F(0.11) DF 1,12, p=0.74]. D) Rosa^{tdTomato} and PTEN$^{f/f}$;Rosa^{tdTomato} mice were injected with 6E9 GC/mouse of AAV/Cre. Two-way repeated measures ANOVA revealed significant differences over time [F(988.0) DF 5.13, 123.1, p<0.0001] and no significant differences in grip strength between genotypes [F(4.24) = DF 1,24, p=0.051]. E-F) Two-way repeated measures ANOVA revealed no significant sex differences for the Rosa^{tdTomato} mice [F(3.17) DF 1,10, p=0.11] nor for the PTEN$^{f/f}$;Rosa^{tdTomato} mice [F(0.42) DF 1,12, p=0.53].

670

671 3.2.5. Study 5: PTEN deletion only in local spinal circuitry:

672 Study 5 tested whether pathophysiologies were due to deletion of PTEN in local
673 spinal cord circuitry in the context of a spinal cord injury. Mice received dorsal
674 hemisection injuries and intra-spinal cord injections of AAV2/Cre rather than AAV-rg/Cre
675 (6E9 GC/mouse). Intra-spinal injections of AAV2/Cre delete PTEN in a local region of
676 the spinal cord around the injection site (Fig. 5D) but there is no retrograde transduction
677 of cells of origin of spinal pathways in the brain. PTEN$^{f/f}$;Rosa^{tdTomato} mice received 2
678 injections above the level of the dorsal hemisection at approximately C4. Controls were
679 Rosa^{tdTomato} mice that received similar injections. Forelimb motor function was assessed
680 over time using a GSM by an individual blinded to treatment group.

681 Following C5 lesions and AAV2/Cre intra-spinal cord injections, 7 days post-injury
682 GSM values dropped to 8.3% of pre-injury values for Rosa^{tdTomato} mice and 1.8% of pre-
683 injury values for PTEN$^{f/f}$;Rosa^{tdTomato} mice. Values remained low for the duration of the
684 testing period and they plateaued at around 21 days post injury to 5.4% of pre-injury
685 control and to 2.6% of pre-injury values for PTEN$^{f/f}$;Rosa^{tdTomato} mice. Two-way repeated
686 measures ANOVA revealed significant differences over time [F(988.0) DF 5.13, 123.1,
687 $p<0.0001$] and no significant differences in grip strength between genotypes [F(4.24) =
688 DF 1,24, $p=0.051$].

689

690 3.2.5.a. Comparisons by sex:

691 Stratification of GSM data by sex (Fig. 5E &F) revealed no sex differences in the
692 values of the Rosa^{tdTomato} control mice or in the values of the PTEN$^{f/f}$;Rosa^{tdTomato} mice

693 injected with AAV2/Cre. Specifically, at 21 days post injury, GSM values for female
694 PTEN$^{f/f}$;Rosa^{tdTomato} mice (PTEN-deleted) were 2.7% of pre-injury control at the plateau
695 vs. 7.7% for the Rosa^{tdTomato} female control mice. GSM values for male
696 PTEN$^{f/f}$;Rosa^{tdTomato} mice were 1.7% of pre-injury control at the plateau vs. 1.5% for the
697 Rosa^{tdTomato} male control mice. Two-way repeated measures ANOVA revealed no
698 significant sex differences for the Rosa^{tdTomato} mice [F(3.17) DF 1,10, p=0.11] nor for the
699 PTEN$^{f/f}$;Rosa^{tdTomato} mice [F(0.42) DF 1,12, p=0.53]. Overall neither group showed
700 improvement in recovery of function after SCI plus AAV2/Cre intraspinal injections.
701
702 3.2.5.b. Late-developing pathophysiologies:
703 None of the mice that received dorsal hemisections and intra-spinal injections of
704 AAV2/Cre (non-retrograde) exhibited pathophysiologies described above. All animals
705 were euthanized 42 days post injury.
706
707 3.2.6. Retrospective analysis of whether there are pathophysiologies with intra-spinal
708 injections of AAV-rg/Cre without concurrent SCI:
709 To assess whether pathophysiologies developed with injections of AAV-rg/Cre
710 without concurrent SCI, we reviewed husbandry and survival records from mice in our
711 previous anatomical studies assessing retrograde transduction via AAV-rg/Cre
712 (Metcalfe et al., 2022; Steward et al., 2021). These studies involved 12
713 PTEN$^{f/f}$;Rosa^{tdTomato} mice (n=8 males; n=3 females) that were allowed to survive for
714 different intervals after bilateral intra-spinal cord injections of AAV-rg/Cre at C5 (6E9
715 GC/mouse). Three mice (2 males and 1 female) survived for 1 month post AAV-rg/Cre

716 injection; 4 males survived 4 months post AAV-rg/Cre injection; 1 male survived 7
717 months post AAV-rg/Cre injection; 5 mice (n=2 males and n=3 females) survived 12
718 months post AAV-rg/Cre injection. None of these mice exhibited scratching or hindlimb
719 dystonia or any other adverse condition that led to euthanasia.
720

721 **3.3. Transduction of DRG neurons:**

722 The incessant scratching that develops suggests pathological itch, which can be due
723 to sensitization of acute itch pathways that originate from defined populations of DRG
724 neurons (Akiyama and Carstens, 2013). Accordingly, we were curious whether DRG
725 neurons that have been implicated in pathological itch are retrogradely transduced. We
726 have previously shown that medium-sized neurons in DRGs within a few segments of
727 the injection site at C5 are retrogradely transduced and that these are not CGRP-
728 positive nociceptors (Metcalfe et al., 2022).

729 One recent study reported that PTEN deletion in isolectin B4 (IB4)-positive DRG
730 neurons in adult mice, promotes ectopic TRPV1 and Mrgpr3a expression leading to
731 pathological itch (Hu et al., 2022). Sensory representation of the neck and ears is
732 represented at C3, so injections of AAV-rg/Cre at C5 could transduce DRG neurons at
733 C3, deleting PTEN in sensory neurons that innervate the neck and head. This
734 mechanism could account for the incessant scratching we observe if IB4-positive
735 neurons in the DRG are transduced by AAV-rg/Cre injections into the spinal cord.

736 To rule in or rule out this possible mechanism, we assessed retrograde transduction
737 of DRG neurons from mice in Study 1. Slide-mounted cross-sections from spinal
738 segments near the injection site with DRGs were stained for IB4 and co-imaged for tdT

739 and imaged to assess co-labeling. Many medium sized DRG neurons were tdT positive,
740 there were no convincing examples of co-labeling with IB4 (Fig. 6). This finding does
741 not support the hypothesis that excessive scratching is due to PTEN deletion in IB4-
742 expressing DGR neurons.

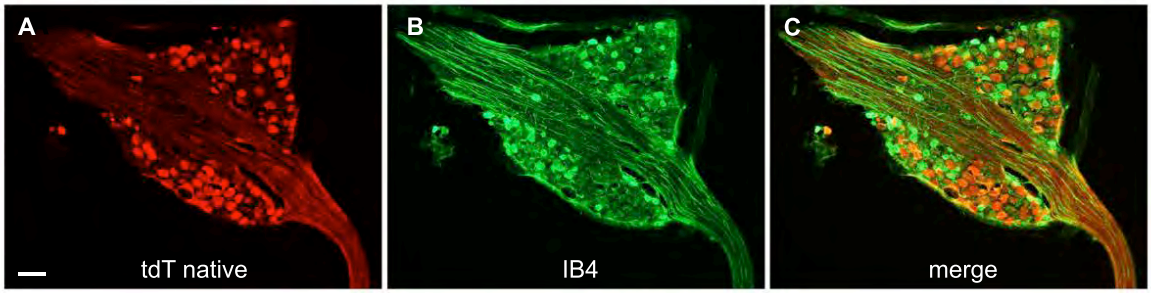

743

Figure 6. Intraspinal AAV-rg injections transduce DRG neurons with no transduction of IB4+ neurons. A) tdT-positve DRG neurons in PTEN$^{f/f}$;Rosa^{tdTomato} mice. B). IHC for isolectin B4 (IB4)-positive DRG neurons. C) Merge of A) and B) tdT-positive DRG neurons expressing IB4 (if present) would be yellow (none are evident). Scale bar (100 μm).

744 Another possible circuit for persistent itch involves the mechanical itch pathway (Pan
745 et al., 2019). First order neurons for this circuit are toll-like receptor 5-positive DRG
746 neurons (TLR5+) that give rise to low-threshold mechanoreceptors. These DRG
747 neurons project to a population of Urocortin-3 expressing (Unc3+) excitatory
748 interneurons in the dorsal horn. Thus, a possible mechanism for chronic itch would be
749 increased intrinsic excitability of TLR5+ DRG neurons due to PTEN deletion. As above,
750 this could only occur if this population of DRG neurons is transduced by AAV-rg/Cre
751 injections into the spinal cord. To rule in or rule out this mechanism, slide-mounted
752 cross-sections from DRGs near the injection site with DRGs were stained using what
753 was presumably the same TLR5 antibody from Santa Crus that had been used by (Pan
754 et al., 2019). Although we tried several different immunostaining procedures, we were
755 unable to replicate the findings of Pan et al. in which a select population of DRG
756 neurons were positive for TLR5. Instead, almost all DRG neurons exhibited weak

757 immunofluorescence (data not shown). Because our immunostaining did not reveal a
758 subset of DRG neurons that were selectively labeled for TLR5, it remains possible that
759 some of the DRG neurons transduced by AAV-rg are first order neurons of the
760 mechanical itch pathway.
761

762 **4. DISCUSSION**

763 The overall goal of this study was to evaluate AAV-rg as a potential platform to
764 promote motor recovery after cervical SCI by deleting PTEN in multiple pathways. Our
765 results revealed: 1) Intra-spinal cord injections of AAV-rg/Cre at the time of a dorsal
766 hemisection at C5 in PTEN$^{f/f}$;Rosa^{tdTomato} mice enhanced forelimb motor recovery in a
767 dose (GC) dependent fashion. 2) There were major sex differences in the extent of
768 recovery. Male mice exhibited much greater recovery than females, and the data from
769 males largely accounted for the differences in the combined data. 3) Despite initial
770 recovery, late-onset pathophysiologies involving incessant scratching and hindlimb
771 dystonia developed in many mice, compromising the motor recovery. 4) Development of
772 pathophysiologies was dose-dependent, but pathophysiologies occurred even at low
773 GC doses that did not enhance recovery. 5) Pathophysiologies were also seen with
774 AAV-rg/shPTEN injections at C5, although the GC does used did not enhance motor
775 recovery. 6) Pathophysiologies were not seen with injections of AAV2/Cre at C5 (not
776 retro) or with injections of AAV-rg/Cre without concurrent SCI. In what follows, we
777 discuss implications and caveats of these results.
778

779 **<u>4.1. Dose-dependence for enhanced recovery:</u>**

780 Previous studies have reported that PTEN deletion in the sensorimotor cortex can
781 enhance axonal regeneration and functional recovery after spinal cord injury (Danilov
782 and Steward, 2015; Du et al., 2015; Geoffroy et al., 2015; Lewandowski and Steward,
783 2014; Liu et al., 2010; Zukor et al., 2013). PTEN is a phosphatase that negatively
784 regulates the PI3K/AKT/mTOR signaling pathway, which is crucial for neuronal survival,
785 axonal growth, and regeneration (Leibinger et al., 2019; Proud, 2002; Testa and
786 Tsichlis, 2005; Zhou and Snider, 2006). The present study extends the story by
787 demonstrating that PTEN deletion via retrograde transduction using AAV-rg/Cre can
788 also enhance motor recovery.
789 Enhanced recovery of forelimb motor function with intra-spinal injections of AAV-
790 rg/Cre at the time of injury was dose-dependent. Recovery was seen at higher doses
791 12E9 and 6E9 GC (genome copies) and was not seen with the lowest dose tested (3E9
792 GC). Counts of PTEN-deleted cortical motoneurons (ghost cells in layer V of the
793 sensorimotor cortex) revealed dose-dependent differences in the numbers of PTEN-
794 deleted neurons in Layer V between high and intermediate GC doses.
795 The likely explanation for the small difference in the numbers of PTEN-negative cells
796 between the high and intermediate GC doses is that the high dose involved 4 injections,
797 2 rostral and 2 caudal to the injury. Since the dorsal and dorso-lateral CST is completely
798 transected by a dorsal hemisection, injections below the injury would not be expected to
799 transduce many CMNs. One possible explanation for the better outcome in functional
800 recovery at high doses could be that AAV-rg/Cre injections below the injury may be
801 promoting rewiring and synaptic plasticity of intraspinal circuitry. Recent studies have
802 shown that coordinated growth stimulation in supra spinal centers and in spinal relay

803 stations led to enhancement in neuronal rewiring and improved locomotor recovery
804 (Van Steenbergen et al., 2023). The combination of these effects may elicit a greater
805 recovery of function than what is observed with intermediate doses of AAV-rg/Cre.
806

807 **4.3. Sex differences in functional recovery of PTEN-deleted mice after SCI:**

808 Our results also demonstrate major sex differences in the response to AAV-rg-
809 mediated PTEN deletion following dorsal hemisection injury in that male mice exhibited
810 much greater recovery than females. Several studies have investigated sex-related
811 differences in functional recovery after SCI in animal models. For instance, female
812 C57Bl/6 mice with thoracic-level compression injuries have shown better locomotor
813 scores and less necrosis and inflammatory cell infiltration than males (Farooque et al.,
814 2006). Additionally, female mice showed significantly better recovery than males after a
815 moderate compression SCI (Hauben et al., 2002). It is worth noting that these studies
816 used compression injuries that can lead to a secondary inflammatory response, which is
817 not as extensive in transection models as used in our study (Watanabe et al., 1999). It
818 is possible that the better outcomes observed in female mice in other studies may be
819 attributed to neuroprotective roles of estrogen-like hormones in the CNS (Yune et al.,
820 2004).

821 Sex differences in neurologic recovery have been observed in clinical studies of
822 humans, with females showing greater natural recovery than males. However, at the
823 time of discharge from rehabilitation, males tend to perform better functionally for a
824 given level and degree of neurologic injury (Sipski et al., 2004). The underlying reasons
825 for these sex differences are not yet fully understood and could involve a range of

826 factors such as hormone levels, genetics, or other factors. Further studies are needed
827 to elucidate the mechanisms underlying these differences, which could ultimately lead
828 to the development of more effective treatments for spinal cord injury in both males and
829 females.

830 **4.4. Late onset pathophysiologies:**

831 Despite enhanced motor recovery with AAV-rg-mediated PTEN deletion, many mice
832 exhibited pathophysiologies with all doses used in this study, even low doses that did
833 not elicit functional recovery. Late-onset pathophysiologies occurred only with AAV-rg
834 based delivery of PTEN modifiers (AAV-rg/Cre or AAV-rg/shPTEN/GFP) in conjunction
835 with SCI (dorsal hemisection at C5). This finding suggests several conclusions. 1)
836 Pathophysiologies are not due to PTEN-deletion in spinal circuitry only. This conclusion
837 is supported by the fact that animals that received intraspinal AAV2/Cre injections to
838 delete PTEN in local spinal circuitry ($PTEN^{f/f}$;$Rosa^{tdT}$ + AAV2/Cre + SCI) did not show
839 scratching or hindlimb dystonia. 2) Pathophysiologies are not due to PTEN-deletion
840 alone, since PTEN deleted animals without SCI ($PTEN^{f/f}$;$Rosa^{tdT}$ + AAV-rg/Cre - SCI)
841 do not exhibit pathophysiologies. Although mice that received AAV2/Cre without injury
842 did not exhibit excessive scratching sufficient to cause skin injury, we did not assess
843 scratching behavior directly and so cannot exclude increased scratching with spinal
844 cord PTEN deletion as reported by (Hu et al., 2022).

845 Some PTEN-deleted animals that received cervical SCI also exhibited rigid forward
846 extension of the hindlimbs (dystonia). Dystonias can be caused by loss of descending
847 inputs. Clinicians use the term "upper motoneuron lesions", and the explanation is that
848 there is net loss of descending inhibition spinal circuits, resulting in hyperactivity

849 (Bakheit et al., 2011; Sheean and McGuire, 2009). Transduction of CMNs with
850 intraspinal spinal AAV-rg/Cre could disrupt their physiological activity producing
851 functional phenotypes similar to “upper motoneuron lesions”.
852 Hindlimb dystonias could be also driven by altered connections entirely within the
853 injured spinal cord, again with the constraint that these only occur with PTEN deletion
854 via AAV-rg in conjunction with SCI. The incessant scratching is with the hindlimb, so it
855 is plausible that what begins as an “itch phenotype” converts to hindlimb dystonia driven
856 by the lumbar spinal cord. Future studies will be required to explore these possible
857 mechanisms.
858 One important clue regarding possible mechanisms is that pathophysiologies are not
859 observed with deletion of PTEN limited to local spinal circuitry (AAV2/Cre rather than
860 AAV-rg/Cre or AAV-rg/shPTEN). This suggests that the pathophysiologies may be due
861 to retrograde transduction and PTEN deletion in neurons that project to the area of the
862 AAV-rg injection. These could include cells of origin any of the descending pathways
863 from the brain, cells of origin of intra-spinal pathways including second order sensory
864 neurons, or first order DRG neurons that give rise to ascending sensory pathways.
865 A second clue regarding possible mechanisms of the pathophysiologies is that they
866 appear after some delay (4-5 weeks) and increase in incidence and severity over time.
867 This time delay suggests a mechanism that evolves over time, reaching a threshold that
868 triggers aberrant behaviors. Possible explanations include: 1) Growth induced by PTEN
869 deletion leading to the formation of aberrant connections; 2) Persistent activation of the
870 mTOR signaling pathway, which can have profound consequences on the physiological

871 properties of neurons, including causing seizures (Backman et al., 2001; LaSarge et al.,
872 2021; Ogawa et al., 2007; Pun et al., 2012).
873
874 **4.5. Transduction of DRG neurons:**
875 In our previous studies involving intra-spinal AAV-rg/Cre injections, we observed
876 retrograde transduction of large DRG neurons in dorsal root ganglia within a few
877 segments of the injection site at C5 (Metcalfe et al., 2022). Sensory representation of
878 the neck and ears is represented at C3, and it is possible that injections of AAV-rg/Cre
879 at C5 transduce some DRG neurons at C3, therefore eliciting PTEN deletion in sensory
880 neurons that innervate the neck and head.
881 The incessant scratching that develops suggests the possibility of chronic itch in the
882 region of the neck and head. Rodents and other quadrupeds use their hindlimbs to
883 scratch regions of their upper torso, neck, and head to relieve itch or sometimes in
884 response to other sensations. In some pathological conditions, chronic itch is caused by
885 peripheral and central sensitization of acute itch pathways, with sensitization of itch-
886 related somatosensory pathways in DRG neurons (Akiyama and Carstens, 2013).
887 Although both mechanical and chemical itch trigger site-directed scratching, these
888 two forms are transmitted through different neural circuits. Recent studies have found
889 that interneurons in the dorsal spinal cord expressing urocortin 3 (Ucn3+) (Pan et al.,
890 2019) and neuropeptide Y receptor (Y1R+) (Acton et al., 2019) are essential for
891 transmitting mechanical itch, and they receive inputs from Toll-like receptor 5-positive
892 (TLR5+) Aß low-threshold mechanoreceptors (LTMR). Downstream projection circuits
893 remain unknown. Itch-inducing molecules activate several membrane-bound receptors,

894 such as histamine receptors (Rossbach et al., 2009). Recently, the Mas-related G-
895 protein coupled receptor (Mrgpr) (Liu et al., 2009) and the transient receptor potential
896 (TRP) channel subfamily V member 1 (TRPV1) (Davidson and Giesler, 2010) have
897 been reported to be required for processing the histamine-induced itch response
898 (Davidson and Giesler, 2010). At the spinal level, secondary neurons for pruriceptors
899 express gastrin-releasing peptide (GRP) in the spinal dorsal horn (Bautista et al., 2014;
900 Sun et al., 2017; Sun and Chen, 2007). Information is then transmitted to spinal tertiary
901 pruriceptors expressing the GRP receptor (GRPR). Finally, this information is
902 transmitted to supraspinal regions via a relay of spinal ascending neurons (Mu et al.,
903 2017). It remains to be seen whether any of these neuron types and pathways are
904 transduced by intra-spinal injections of AAV-rg/Cre, and if they are, how consequences
905 could differ in the context of SCI.

906 Our previous studies with cervical intraspinal injections of AAV-rg/Cre revealed that
907 retrogradely transduced neurons in the DRG (identified by tdT labeling) are distinct from
908 the population neurons that express calcitonin gene-related peptide (CGRP) that
909 mediate nociception (meaning no-co-expression was detected) (Metcalfe et al., 2022).
910 Here, we carried out initial studies to test whether AAV-rg transduced DRG neurons
911 expressing markers of either itch pathway.

912 To test for transduction of TLR5 neurons, we used what was presumably the same
913 TLR5 antibody from Santa Crus that had been used by Pan et al., 2019. However, we
914 were unable to replicate the findings that a select population of DRG neurons were
915 positive for TLR5. We were unable to determine the RRID for either the antibody used
916 by Pan et al or the one we used, so it is possible that the antibodies from Santa Cruz

917 are from a different batch. Because our immunostaining did not reveal a subset of DRG
918 neurons that were selectively labeled for TLR5, it remains possible that some of the
919 DRG neurons transduced by AAV-rg are first order neurons of the mechanical itch
920 pathway.

921 Another possible pathway for pathological itch is suggested by the recent finding that
922 PTEN deletion in isolectin B4 (IB4)-positive DRG neurons in adult mice, promotes
923 ectopic TRPV1 and Mrgpr3a expression leading to pathological itch (Hu et al., 2022).
924 This mechanism could account for the incessant scratching we observe if IB4-positive
925 neurons are transduced by AAV-rg/Cre injections into the spinal cord. Our results
926 confirmed the presence of a populaton of IB4-expressing DRG neurons, but there were
927 no convincing examples of retrograde transduction evidenced by co-labeling with tdT.
928 This finding does not support the hypothesis that excessive scratching is due to PTEN
929 deletion in IB4-expressing DGR neurons.

930 Within the spinal cord, itch signals are transmitted through the spinothalamic tract
931 and spinobrachial pathway to the thalamus and parabrachial nucleus, respectively,
932 where they are projected to various brain areas for itch processing (Yosipovitch et al.,
933 2018). It remains to be seen whether the second order neurons that give rise to these
934 pathways are transduced by AAV-rg. Descending pathways from various sites modulate
935 transmission along sensory pathways, so it is possible that AAV-rg/Cre-mediated PTEN
936 deletion in the cells of origin of these descending pathways alters itch transmission to
937 trigger pathological scratching. Future studies are needed to explore these possible
938 mechanisms.
939

940 **5. CONCLUSION**

941 Our results support the potential of AAV-rg for enhancing motor recovery after SCI,
942 but also highlight the potential for late-developing pathophysiologies with this approach.
943 A recent study reports other indications of late-developing consequences of AAV-rg-
944 mediated PTEN deletion in a thoracic crush model of SCI. Although AAV-rg/Cre-
945 mediated PTEN deletion resulted in significant initial improvement in locomotor function
946 in comparison to control, improvements were not sustained (Stewart et al., 2023). This
947 highlights the importance of tracking potential long-term consequences of manipulations
948 to enhance axon regeneration after SCI. Further studies are necessary to elucidate the
949 mechanisms underlying late-developing adverse effects and functional deterioration and
950 to determine whether recovery can be achieved without adverse consequences.
951

952 **REFERENCES**
953
954 Acton, D., Ren, X., Di Costanzo, S., Dalet, A., Bourane, S., Bertocchi, I., Eva, C., Goulding, M.,
955 2019. Spinal Neuropeptide Y1 Receptor-Expressing Neurons Form an Essential Excitatory
956 Pathway for Mechanical Itch. Cell Rep 28, 625-639.e626.
957 Akiyama, T., Carstens, E., 2013. Neural processing of itch. Neuroscience 250, 697-714.
958 Backman, S.A., Stambolic, V., Suzuki, A., Haight, J., Elia, A., Pretorius, J., Tsao, M.S., Shannon, P.,
959 Bolon, B., Ivy, G.O., Mak, T.W., 2001. Deletion of Pten in mouse brain causes seizures, ataxia
960 and defects in soma size resembling Lhermitte-Duclos disease. Nat Genet 29, 396-403.
961 Bakheit, A.M., Fheodoroff, K., Molteni, F., 2011. Spasticity or reversible muscle hypertonia? J
962 Rehabil Med 43, 556-557.
963 Bautista, D.M., Wilson, S.R., Hoon, M.A., 2014. Why we scratch an itch: the molecules, cells and
964 circuits of itch. Nat Neurosci 17, 175-182.
965 Challagundla, M., Koch, J.C., Ribas, V.T., Michel, U., Kügler, S., Ostendorf, T., Bradke, F., Müller,
966 H.W., Bähr, M., Lingor, P., 2015. AAV-mediated expression of BAG1 and ROCK2-shRNA promote
967 neuronal survival and axonal sprouting in a rat model of rubrospinal tract injury. J Neurochem
968 134, 261-275.
969 Danilov, C.A., Steward, O., 2015. Conditional genetic deletion of PTEN after a spinal cord injury
970 enhances regenerative growth of CST axons and motor function recovery in mice. Exp Neurol
971 266, 147-160.
972 Davidson, S., Giesler, G.J., 2010. The multiple pathways for itch and their interactions with pain.
973 Trends Neurosci 33, 550-558.
974 Du, K., Zheng, S., Zhang, Q., Li, S., Gao, X., Wang, J., Jiang, L., Liu, K., 2015. Pten Deletion
975 Promotes Regrowth of Corticospinal Tract Axons 1 Year after Spinal Cord Injury. J Neurosci 35,
976 9754-9763.
977 Farooque, M., Suo, Z., Arnold, P.M., Wulser, M.J., Chou, C.T., Vancura, R.W., Fowler, S., Festoff,
978 B.W., 2006. Gender-related differences in recovery of locomotor function after spinal cord
979 injury in mice. Spinal Cord 44, 182-187.
980 Gallent, E.A., Steward, O., 2018. Neuronal PTEN deletion in adult cortical neurons triggers
981 progressive growth of cell bodies, dendrites, and axons. Exp Neurol 303, 12-28.
982 Geoffroy, C.G., Hilton, B.J., Tetzlaff, W., Zheng, B., 2016. Evidence for an Age-Dependent
983 Decline in Axon Regeneration in the Adult Mammalian Central Nervous System. Cell Rep 15,
984 238-246.
985 Geoffroy, C.G., Lorenzana, A.O., Kwan, J.P., Lin, K., Ghassemi, O., Ma, A., Xu, N., Creger, D., Liu,
986 K., He, Z., Zheng, B., 2015. Effects of PTEN and Nogo Codeletion on Corticospinal Axon
987 Sprouting and Regeneration in Mice. J Neurosci 35, 6413-6428.
988 Guertin, D.A., Sabatini, D.M., 2007. Defining the role of mTOR in cancer. Cancer Cell 12, 9-22.
989 Hauben, E., Mizrahi, T., Agranov, E., Schwartz, M., 2002. Sexual dimorphism in the spontaneous
990 recovery from spinal cord injury: a gender gap in beneficial autoimmunity? Eur J Neurosci 16,
991 1731-1740.
992 Hu, L., Jiang, G.Y., Wang, Y.P., Hu, Z.B., Zhou, B.Y., Zhang, L., Song, N.N., Huang, Y., Chai, G.D.,
993 Chen, J.Y., Lang, B., Xu, L., Liu, J.L., Li, Y., Wang, Q.X., Ding, Y.Q., 2022. The role of PTEN in
994 primary sensory neurons in processing itch and thermal information in mice. Cell Rep 39,
995 110724.

996 Kaplitt, M.G., Feigin, A., Tang, C., Fitzsimons, H.L., Mattis, P., Lawlor, P.A., Bland, R.J., Young, D.,
997 Strybing, K., Eidelberg, D., During, M.J., 2007. Safety and tolerability of gene therapy with an
998 adeno-associated virus (AAV) borne GAD gene for Parkinson's disease: an open label, phase I
999 trial. Lancet 369, 2097-2105.
1000 LaSarge, C.L., Pun, R.Y.K., Gu, Z., Riccetti, M.R., Namboodiri, D.V., Tiwari, D., Gross, C., Danzer,
1001 S.C., 2021. mTOR-driven neural circuit changes initiate an epileptogenic cascade. Prog
1002 Neurobiol 200, 101974.
1003 Leibinger, M., Hilla, A.M., Andreadaki, A., Fischer, D., 2019. GSK3-CRMP2 signaling mediates
1004 axonal regeneration induced by Pten knockout. Commun Biol 2, 318.
1005 Lewandowski, G., Steward, O., 2014. AAVshRNA-mediated suppression of PTEN in adult rats in
1006 combination with salmon fibrin administration enables regenerative growth of corticospinal
1007 axons and enhances recovery of voluntary motor function after cervical spinal cord injury. J
1008 Neurosci 34, 9951-9962.
1009 Liu, K., Lu, Y., Lee, J.K., Samara, R., Willenberg, R., Sears-Kraxberger, I., Tedeschi, A., Park, K.K.,
1010 Jin, D., Cai, B., Xu, B., Connolly, L., Steward, O., Zheng, B., He, Z., 2010. PTEN deletion enhances
1011 the regenerative ability of adult corticospinal neurons. Nat Neurosci 13, 1075-1081.
1012 Liu, Q., Tang, Z., Surdenikova, L., Kim, S., Patel, K.N., Kim, A., Ru, F., Guan, Y., Weng, H.J., Geng,
1013 Y., Undem, B.J., Kollarik, M., Chen, Z.F., Anderson, D.J., Dong, X., 2009. Sensory neuron-specific
1014 GPCR Mrgprs are itch receptors mediating chloroquine-induced pruritus. Cell 139, 1353-1365.
1015 Metcalfe, M., Yee, K.M., Luo, J., Martin-Thompson, J.H., Gandhi, S.P., Steward, O., 2022.
1016 Harnessing rAAV-retro for gene manipulations in multiple pathways that are interrupted after
1017 spinal cord injury. Exp Neurol 350, 113965.
1018 Mu, D., Deng, J., Liu, K.F., Wu, Z.Y., Shi, Y.F., Guo, W.M., Mao, Q.Q., Liu, X.J., Li, H., Sun, Y.G.,
1019 2017. A central neural circuit for itch sensation. Science 357, 695-699.
1020 Ogawa, S., Kwon, C.H., Zhou, J., Koovakkattu, D., Parada, L.F., Sinton, C.M., 2007. A seizure-
1021 prone phenotype is associated with altered free-running rhythm in Pten mutant mice. Brain Res
1022 1168, 112-123.
1023 Pan, H., Fatima, M., Li, A., Lee, H., Cai, W., Horwitz, L., Hor, C.C., Zaher, N., Cin, M., Slade, H.,
1024 Huang, T., Xu, X.Z.S., Duan, B., 2019. Identification of a Spinal Circuit for Mechanical and
1025 Persistent Spontaneous Itch. Neuron 103, 1135-1149.e1136.
1026 Park, K.K., Liu, K., Hu, Y., Kanter, J.L., He, Z., 2010. PTEN/mTOR and axon regeneration. Exp
1027 Neurol 223, 45-50.
1028 Park, K.K., Liu, K., Hu, Y., Smith, P.D., Wang, C., Cai, B., Xu, B., Connolly, L., Kramvis, I., Sahin, M.,
1029 He, Z., 2008. Promoting axon regeneration in the adult CNS by modulation of the PTEN/mTOR
1030 pathway. Science 322, 963-966.
1031 Proud, C.G., 2002. Regulation of mammalian translation factors by nutrients. Eur J Biochem 269,
1032 5338-5349.
1033 Pun, R.Y., Rolle, I.J., Lasarge, C.L., Hosford, B.E., Rosen, J.M., Uhl, J.D., Schmeltzer, S.N.,
1034 Faulkner, C., Bronson, S.L., Murphy, B.L., Richards, D.A., Holland, K.D., Danzer, S.C., 2012.
1035 Excessive activation of mTOR in postnatally generated granule cells is sufficient to cause
1036 epilepsy. Neuron 75, 1022-1034.
1037 Rossbach, K., Wendorff, S., Sander, K., Stark, H., Gutzmer, R., Werfel, T., Kietzmann, M.,
1038 Bäumer, W., 2009. Histamine H4 receptor antagonism reduces hapten-induced scratching
1039 behaviour but not inflammation. Exp Dermatol 18, 57-63.

1040 Schneider, C.A., Rasband, W.S., Eliceiri, K.W., 2012. NIH Image to ImageJ: 25 years of image
1041 analysis. Nat Methods 9, 671-675.
1042 Sheean, G., McGuire, J.R., 2009. Spastic hypertonia and movement disorders: pathophysiology,
1043 clinical presentation, and quantification. Pm r 1, 827-833.
1044 Sipski, M.L., Jackson, A.B., Gómez-Marín, O., Estores, I., Stein, A., 2004. Effects of gender on
1045 neurologic and functional recovery after spinal cord injury. Arch Phys Med Rehabil 85, 1826-
1046 1836.
1047 Steward, O., Yee, K.M., Metcalfe, M., Willenberg, R., Luo, J., Azevedo, R., Martin-Thompson,
1048 J.H., Gandhi, S.P., 2021. Rostro-Caudal Specificity of Corticospinal Tract Projections in Mice.
1049 Cereb Cortex 31, 2322-2344.
1050 Stewart, A.N., Kumari, R., Bailey, W.M., Glaser, E.P., Hammers, G.V., Wireman, O.H., Gensel,
1051 J.C., 2023. PTEN knockout using retrogradely transported AAVs restores locomotor abilities in
1052 both acute and chronic spinal cord injury. bioRxiv, 2023.2004.2017.537179.
1053 Sun, S., Xu, Q., Guo, C., Guan, Y., Liu, Q., Dong, X., 2017. Leaky Gate Model: Intensity-
1054 Dependent Coding of Pain and Itch in the Spinal Cord. Neuron 93, 840-853.e845.
1055 Sun, Y.G., Chen, Z.F., 2007. A gastrin-releasing peptide receptor mediates the itch sensation in
1056 the spinal cord. Nature 448, 700-703.
1057 Tervo, D.G., Hwang, B.Y., Viswanathan, S., Gaj, T., Lavzin, M., Ritola, K.D., Lindo, S., Michael, S.,
1058 Kuleshova, E., Ojala, D., Huang, C.C., Gerfen, C.R., Schiller, J., Dudman, J.T., Hantman, A.W.,
1059 Looger, L.L., Schaffer, D.V., Karpova, A.Y., 2016. A Designer AAV Variant Permits Efficient
1060 Retrograde Access to Projection Neurons. Neuron 92, 372-382.
1061 Testa, J.R., Tsichlis, P.N., 2005. AKT signaling in normal and malignant cells. Oncogene 24, 7391-
1062 7393.
1063 Van Steenbergen, V., Burattini, L., Trumpp, M., Fourneau, J., Aljović, A., Chahin, M., Oh, H.,
1064 D'Ambra, M., Bareyre, F.M., 2023. Coordinated neurostimulation promotes circuit rewiring and
1065 unlocks recovery after spinal cord injury. J Exp Med 220.
1066 Wang, Z., Maunze, B., Wang, Y., Tsoulfas, P., Blackmore, M.G., 2018. Global Connectivity and
1067 Function of Descending Spinal Input Revealed by 3D Microscopy and Retrograde Transduction. J
1068 Neurosci 38, 10566-10581.
1069 Watanabe, T., Yamamoto, T., Abe, Y., Saito, N., Kumagai, T., Kayama, H., 1999. Differential
1070 activation of microglia after experimental spinal cord injury. J Neurotrauma 16, 255-265.
1071 Willenberg, R., Zukor, K., Liu, K., He, Z., Steward, O., 2016. Variable laterality of corticospinal
1072 tract axons that regenerate after spinal cord injury as a result of PTEN deletion or knock-down.
1073 n/a-n/a.
1074 Yosipovitch, G., Rosen, J.D., Hashimoto, T., 2018. Itch: From mechanism to (novel) therapeutic
1075 approaches. J Allergy Clin Immunol 142, 1375-1390.
1076 Yune, T.Y., Kim, S.J., Lee, S.M., Lee, Y.K., Oh, Y.J., Kim, Y.C., Markelonis, G.J., Oh, T.H., 2004.
1077 Systemic administration of 17beta-estradiol reduces apoptotic cell death and improves
1078 functional recovery following traumatic spinal cord injury in rats. J Neurotrauma 21, 293-306.
1079 Zhou, F.Q., Snider, W.D., 2006. Intracellular control of developmental and regenerative axon
1080 growth. Philos Trans R Soc Lond B Biol Sci 361, 1575-1592.
1081 Zukor, K., Belin, S., Wang, C., Keelan, N., Wang, X., He, Z., 2013. Short hairpin RNA against PTEN
1082 enhances regenerative growth of corticospinal tract axons after spinal cord injury. J Neurosci
1083 33, 15350-15361.

1084